DOI: 10.1002/ejic.201000357

Platinum Complexes of Aromatic Selenolates

Amy L. Fuller,[a] Fergus R. Knight,[a] Alexandra M. Z. Slawin,[a] and J. Derek Woollins*[a]

Keywords: Platinum / Selenium / Heterocycles

Several synthetic methods are used to prepare naphthalene-based aromatic 1,2-diselenoles. A new one-pot synthesis starting from naphthalene is used to produce the known compound naphtho[1,8-*c*,*d*][1,2]diselenole (Se_2naph). Friedel–Crafts alkylation is used on Se_2naph to substitute either one *tert*-butyl group to form 2-*tert*-butylnaphtho[1,8-*c*,*d*][1,2]diselenole (mt-Se_2naph) or two *tert*-butyl groups to form 2,7-di-*tert*-butylnaphtho[1,8-*c*,*d*][1,2]diselenole (dt-Se_2naph). Bromination of mt-Se_2naph results in dibromination of the naphthalene ring, rather than reaction at selenium, to give 4,7-dibromo-2-*tert*-butylnaphtho[1,8-*c*,*d*][1,2]-diselenole (mt-Se_2naphBr_2). Reduction of the Se–Se bond in Se_2naph, mt-Se_2naph, dibenzo[*c*,*e*][1,2]diselenine (dibenzSe_2), or diphenyl diselenide (Se_2Ph_2) with $LiBEt_3H$, followed by in-situ addition of $[PtCl_2\{P(OPh)_3\}_2]$ yields the four-coordinate mono- and dinuclear platinum(II) bis(phosphite) complexes $[Pt(Se_2naph)\{P(OPh)_3\}_2]$ (**1**), $[Pt(mt\text{-}Se_2naph)\{P(OPh)_3\}_2]$ (**2**), $[Pt_2(dibenzSe_2)_2\{P(OPh)_3\}_2]$ (**3**), *cis*-$[Pt(SePh)_2\{P(OPh)_3\}_2]$ (**4**), and *trans*-$[Pt_2(SePh)_4\{P(OPh)_3\}_2]$ (**5**).

Introduction

The first synthesis of naphtho[1,8-*c*,*d*][1,2]diselenole (Se_2naph) was reported in 1977 by Meinwald et al. (Figure 1).[1] In their work, Se_2naph was synthesized by adding two equivalents of selenium powder to dilithionaphthalene and then exposing the reaction mixture to air to obtain the desired product in 18–22% yield. Today this preparation is still the most referenced procedure for making this compound. In 1988, Yui et al. reported a different synthetic route to Se_2naph, which involves the addition of sodium diselenide (Na_2Se_2) to 1,8-dichloronaphthalene, producing Se_2naph in a 69% yield.[2] Others have started with 1,8-dibromonaphthalene, synthesized 1,8-dilithionaphthalene, then added elemental selenium (as in Meinwald et al.'s procedure); however, low yields are reported (16%).[3] These reported procedures are, in reality, quite lengthy and present a number of synthetic hurdles, i.e. lengthy synthesis of 1,8-dichloro-[4] or 1,8-dibromonaphthalene.[5]

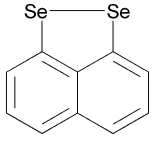

Figure 1. Naphtho[1,8-*c*,*d*][1,2]diselenole (Se_2naph).

In 1994, a synthetic procedure for the sulfur analog, naphtho[1,8-*c*,*d*][1,2]dithiole (S_2naph) was published using unsubstituted naphthalene as a starting material.[6] We have extended that synthesis to the selenium system and developed a facile, "one-pot" synthesis for Se_2naph. We have investigated substitution of this ring using Friedel–Crafts alkylation and report the synthesis of 2,7-di-*tert*-butylnaphtho[1,8-*c*,*d*][1,2]diselenole (dt-Se_2naph) and 2-*tert*-butylnaphtho[1,8-*c*,*d*][1,2]diselenole (mt-Se_2naph). Reaction of mt-Se_2naph with bromine gives 4,7-dibromo-2-*tert*-butylnaphtho[1,8-*c*,*d*][1,2]diselenole (mt-Se_2naphBr_2) (Figure 2).

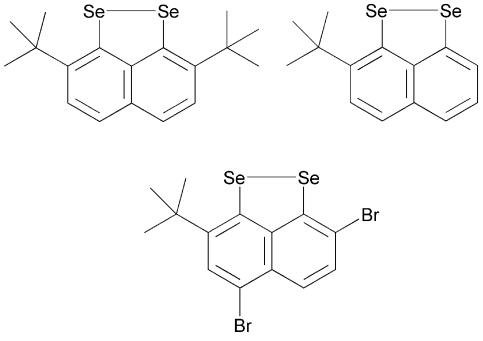

Figure 2. 2,7-di-*tert*-butylnaphtho[1,8-*c*,*d*][1,2]diselenole (dt-Se_2naph), 2-*tert*-butylnaphtho[1,8-*c*,*d*][1,2]diselenole (mt-Se_2naph), and 4,7-dibromo-2-*tert*-butylnaphtho[1,8-*c*,*d*][1,2]diselenole (mt-Se_2naphBr_2).

The crystal structure of Se_2naph has previously been reported,[7] along with several other compounds having an Se–Se bond; such as dibenzo[*c*,*e*][1,2]diselenine (dibenzSe_2) and diphenyl diselenide (Se_2Ph_2) (Figure 3).[8,9] Similar backbones in each of these compounds produce similar chemical environments for the selenium atoms. Although the compounds are structurally similar around the selenium atoms, there are major differences in the conformation that the backbone forces on the selenium substituents. As a result, the Se–Se bond length varies as a function of the flexi-

[a] School of Chemistry, University of St Andrews, St Andrews, Fife KY16 9ST, UK
E-mail: jdw3@st-and.ac.uk

bility of the diaryl backbone. Se_2naph has the longest Se–Se bond length at 2.3639(5) Å, followed by dibenzo[*c*,*e*][1,2]-diselenine (benzSe_2) [2.323(2) Å], and then diphenyl diselenide (Se_2Ph_2) [2.29(1) Å]. The direct relationship that can be drawn is the more rigid the backbone, the longer the Se–Se bond.

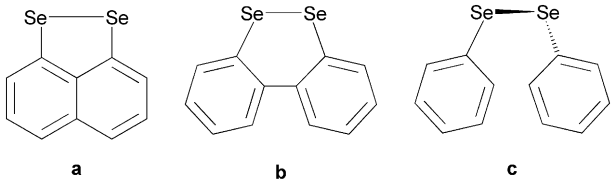

Figure 3. **a**: Naphtho[1,8-*c*,*d*][1,2]diselenole (Se_2naph), **b**: dibenzo-[*c*,*e*][1,2]diselenine (dibenzSe_2), and **c**: diphenyl diselenide (Se_2Ph_2).

These compounds can be used as ligands, by reducing the Se–Se bond to form dianionic *Se₂naph* or *dibenzSe₂* or monoanionic *SePh* (the reduced, negatively charged ligands are indicated by italics). There are very few metal complexes reported that have *Se₂naph* (or any naphthalene derivative) or *dibenzSe* as a ligand. These are limited to the platinum(II) bis(phosphane) complexes, [Pt(*Se₂naph*)(PPh_3)$_2$], [Pt(*Se₂naph*)(PMe_3)$_2$], and [Pt(*dibenzSe₂*)(PPh_3)$_2$].[10,11] Furthermore, there are only a few reported mononuclear square-planar complexes having two *SePh* ligands. These include *cis*- and *trans*-[Pt(*SePh*)$_2$(PPh_3)$_2$], *trans*-[Pt(*SePh*)$_2${P(*n*Bu)$_3$}$_2$], and *trans*-[Pt(*SePh*)$_2$(PEt_3)$_2$]. Not only does *SePh* form mononuclear complexes, but there are several examples of the formation of dinuclear complexes with *SePh* moieties bridging the two metal centers (Figure 4).[11–13]

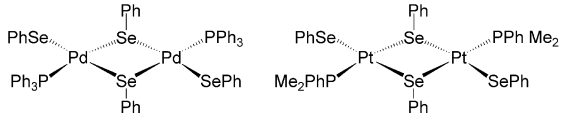

Figure 4. Known dinuclear complexes with bridging SePh ligands.

To date, there is only one reported "series" of related complexes. This series contains platinum bis-triphenylphosphane complexes with the general formula LPt(PPh_3)$_2$, where L is *Se₂naph*, *dibenzSe₂*, or two molecules of *SePh* (Figure 5). These complexes were not synthesized in a single laboratory, but have been reported independently by several groups. [Pt(PPh_3)$_2$(*Se₂naph*)], [Pt(PPh_3)$_2$(*dibenzSe₂*)], and *cis*-[Pt(PPh_3)$_2$(*SePh*)$_2$] were obtained via oxidative addition reactions with [Pt(PPh_3)$_4$] and the respective neutral diselenium compound.[10,11,14] These complexes are very similar around the Pt^{II} metal center despite the flexibility of the backbone.

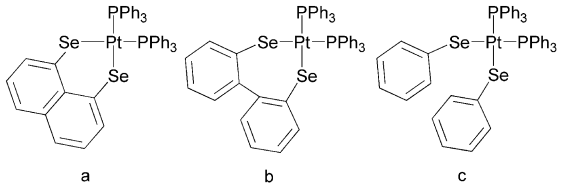

Figure 5. **a**: [Pt(PPh_3)$_2$(Se_2naph)], **b**: [Pt(PPh_3)$_2$(dibenzSe_2)], and **c**: *cis*-[Pt(PPh_3)$_2$($SePh)_2$].

In order to expand the number of di-selenium containing complexes and to obtain a series of these types of platinum complexes from which to draw structural insights, we have synthesized and characterized a new group of complexes produced by reactions using *cis*-[$PtCl_2${P(OPh)$_3$}$_2$] as a starting material. The resulting four-coordinate mono- and di-nuclear platinum(II) bis-phosphite complexes are [Pt(*Se₂naph*){P(OPh)$_3$}$_2$] (**1**), [Pt(*mt-Se₂naph*){P(OPh)$_3$}$_2$] (**2**), [Pt_2(*dibenzSe₂*)$_2${P(OPh)$_3$}$_2$] (**3**), *cis*-[Pt(*SePh*)$_2${P(OPh)$_3$}$_2$] (**4**), and *trans*-[Pt_2(*SePh*)$_4${P(OPh)$_3$}$_2$] (**5**) (Figure 6). The X-ray structures of these compounds are reported along with a detailed comparison of their structures focusing on the geometry around the Pt^{II} metal center.

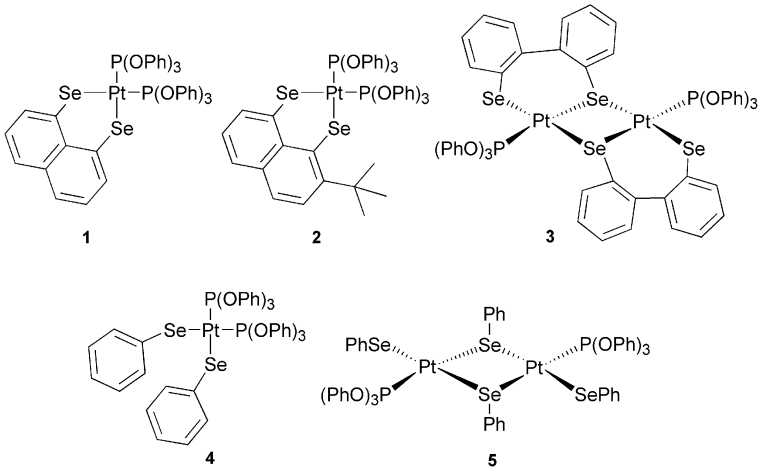

Figure 6. Complexes reported in this work: [Pt(*Se₂naph*){P(OPh)$_3$}$_2$] (**1**), [Pt(*mt-Se₂naph*){P(OPh)$_3$}$_2$] (**2**), [Pt_2(*dibenzSe₂*)$_2${P(OPh)$_3$}$_2$] (**3**), *cis*-[Pt(*SePh*)$_2${P(OPh)$_3$}$_2$] (**4**) and *trans*-[Pt_2(*SePh*)$_4${P(OPh)$_3$}$_2$] (**5**).

Results and Discussion

Several useful ligands have been prepared by novel synthetic methods in the course of this research. Naphtho[1,8-*c*,*d*][1,2]diselenole (Se_2naph) is synthesized using a one-pot reaction starting from naphthalene (26% yield). This synthesis was modelled after one reported by Ashe et al. for the sulfur analog naphtho[1,8-*c*,*d*][1,2]dithiole.[6] It was also found that substitution of the naphthalene ring in Se_2naph with either one *tert*-butyl group to form 2-*tert*-butylnaphtho[1,8-*c*,*d*][1,2]diselenole (mt-Se_2naph) or two *tert*-butyl groups to form 2,7-di-*tert*-butylnaphtho[1,8-*c*,*d*][1,2]diselenole (dt-Se_2naph) was possible via a standard Friedel–Crafts alkylation.[7,15] The addition of dibromine to mt-Se_2naph gave no reaction between selenium and bromine. Instead, electrophilic aromatic substitution dominates to produce the doubly substituted compound 4,7-dibromo-2-*tert*-butylnaphtho[1,8-*c*,*d*][1,2]diselenole (mt-Se_2naphBr_2) (Scheme 1). This is unusual, since reacting organoselenium compounds with dibromine generally results in oxidative addition with addition of the dibromine to the selenium atom, which adopts a "T-shaped" geometry.[16–18]

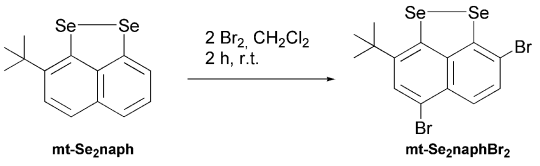

Scheme 1. The reaction scheme for the preparation of 4,7-dibromo-2-*tert*-butylnaphtho[1,8-*c*,*d*][1,2]diselenole (mt-Se_2naphBr_2).

The bromine selectivity can be explained by the electronic directing influence of selenium and the steric bulk of the *tert*-butyl group. Both selenium and *tert*-butyl groups donate electrons into the π-system, activating the naphthalene ring and directing incoming electrophiles to the *ortho* or *para* positions. The first attack at the position *para* to selenium would be sterically more favorable, keeping the two large bromine and *tert*-butyl groups further apart. However, the second substitution reaction is directed to the *ortho* position on the second ring to avoid the steric interaction with the first bromine atom.

A unique characteristic of these compounds is the selenium NMR spectroscopy. These compounds are made up of ^{77}SeSe, Se^{77}Se, and ^{77}Se^{77}Se isotopomers. Any selenium sample is a mixture of several stable isotopes, but only ^{77}Se, natural abundance of 7%, is NMR active. When the selenium atoms are in different chemical environments, the ^{77}Se NMR contains two major signals. For example, in mt-Se_2naph, the first two isotopomers give rise to singlets centered at 414 and 360 ppm, whilst the latter gives an AX spectrum with $J_{Se\text{-}Se}$ = 345 Hz (Figure 7). The peak at δ = 360 ppm corresponds to the selenium atom closest to the *tert*-butyl group, based on comparison to the ^{77}Se spectra of Se_2naph (δ = 420 ppm) and dt-Se_2naph (δ = 353 ppm). The ^{77}Se NMR spectrum of mt-Se_2naphBr_2, is similar, showing two shifts at 454 and 374 ppm, however, the peaks were broad and the $J_{Se\text{-}Se}$ could not be determined.

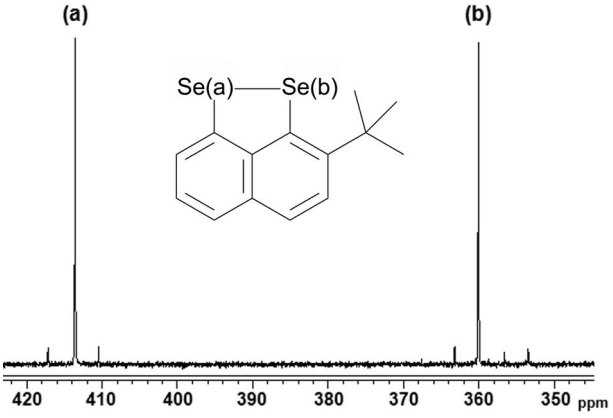

Figure 7. The ^{77}Se NMR for mt-Se_2naph.

X-ray structural characterization was conducted for dt-Se_2naph and mt-Se_2naphBr_2 (Table 1, Figure 8), however, mt-Se_2naph is a persistent oil and could not be crystallized.

Table 1. Selected interatomic distances [Å] and angles [°] for dt-Se_2naph and mt-Se_2naphBr_2.

	dt-Se_2naph[a]	mt-Se_2naphBr_2
Se(1)–Se	2.3383(5)	2.3388(14)
Se(1)–C(1)	1.934(3)	1.935(9)
Se(2)–C(9)		1.888(9)
Se(1)–Se(2)–C(9)		90.9(3)
Se(2)–Se(1)–C(1)	93.16(10)	93.9(2)
Se(1)–C(1)–C(2)	122.4(2)	122.0(7)
Se(1)–C(1)–C(10)	113.2(2)	114.4(6)
Se(2)–C(9)–C(8)		121.6(7)
Se(2)–C(9)–C(10)		119.1(7)
C(2)–C(1)–C(10)	124.3(3)	123.6(8)
C(10)–C(9)–C(8)		119.3(8)
C(1)–C(10)–C(9)	124.8(3)	121.7(8)
C(4)–C(5)–C(10)–C(1)	–0.9(2)	–1.0(5)
C(6)–C(5)–C(10)–C(9)	–0.9(2)	–1.0(5)
C(4)–C(5)–C(10)–C(9)	179.1(2)	180.0(10)
C(6)–C(5)–C(10)–C(1)	179.1(2)	180.0(10)
Mean plane deviations		
Se(1)	–0.1989(57)	–3.2451(39)
Se(2)		–3.3015(40)

[a] Se(2) is Se(1A), C(10) is C(6), C(9) is C(1A) and C(6) is C(4A)′.

The Se–Se bond lengths of dt-Se_2naph [2.3383(5) Å] and mt-Se_2naphBr_2 [2.3388(14) Å] are almost identical, but they are shorter than in Se_2naph, [2.3639(5) Å].[7] In dt-Se_2naph the selenium atoms are forced out of the plane, but this does not occur in Se_2naph or mt-Se_2naphBr_2. Despite the deviation from planarity of dt-Se_2naph, a comparison of torsion angles around the bridgehead carbon atoms of the backbone reveals little variation between Se_2naph, dt-Se_2naph and mt-Se_2naphBr_2 (Figure 9).

The crystal packing in Se_2naph, dt-Se_2naph and mt-Se_2naphBr_2 shows significant differences. Se_2naph forms herringbone π-stacks that are linked by an Se···Se interaction, with a π-π distance between naphthalene rings on

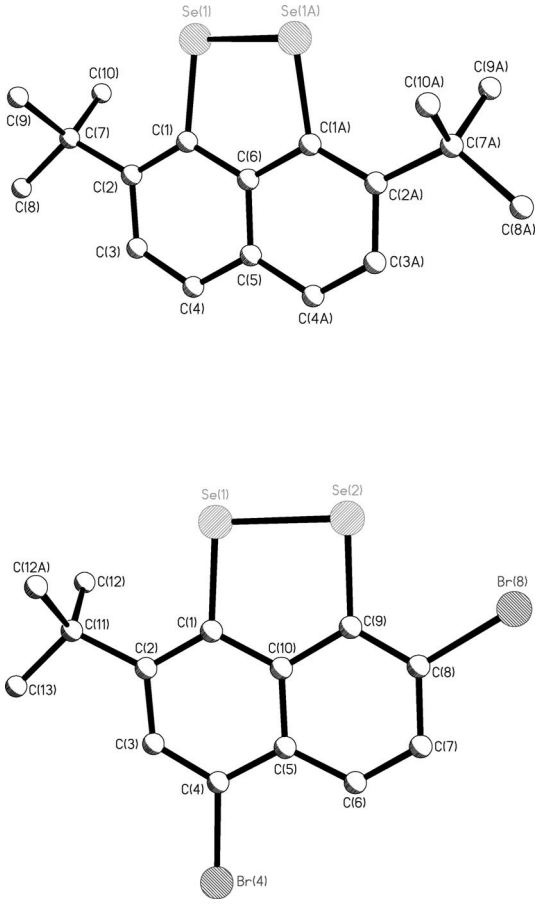

Figure 8. Molecular representation of mt-Se_2naph (top) and mt-Se_2naphBr_2 (bottom).

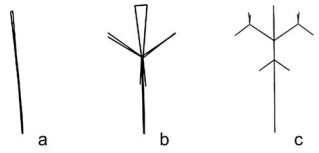

Figure 9. Out-of-plane deflections of a) Se_2naph, b) dt-Se_2naph, and c) mt-Se_2naphBr_2.

separate molecules of 3.81 Å.[7] However, due to the bulky *tert*-butyl arms, there are no intermolecular interactions between Se atoms in the crystal packing of dt-Se_2naph. In mt-Se_2naphBr_2, there is no intermolecular Se···Se interaction, however, there is a close intermolecular Br(4)···Br(8)′ contact [3.4790(13) Å]. This interaction and the resulting packing, is illustrated in Figure 10.

Reduction of the Se–Se bond in Se_2naph, mt-Se_2naph, or dibenzo[*c*,*e*][1,2]diselenine (dibenzSe_2) forms the dianion of those species {the presence of which, is denoted by italics in a molecular formula, e.g. [Pt(*mt-Se*$_2$*naph*)(P(OPh)$_3$)$_2$]}. The analogous reduction of diphenyl diselenide (Se_2Ph_2) gives monoanionic *SePh* (also indicated by italics). Formation of the anion is followed by in situ addition of [$PtCl_2${P(OPh)$_3$}$_2$], which yield the four-coordinate mono- and di-nuclear platinum(II) bis-phosphite complexes [Pt(*Se*$_2$*naph*){P(OPh)$_3$}$_2$] (**1**), [Pt(*mt-Se*$_2$*naph*){P(OPh)$_3$}$_2$] (**2**), [Pt$_2$(*dibenzSe*$_2$)$_2${P(OPh)$_3$}$_2$] (**3**), *cis*-[Pt(*SePh*)$_2${P(OPh)$_3$}$_2$] (**4**), and *trans*-[Pt$_2$(*SePh*)$_4${P(OPh)$_3$}$_2$] (**5**). Scheme 2 shows the reaction to form **1** and **2**.

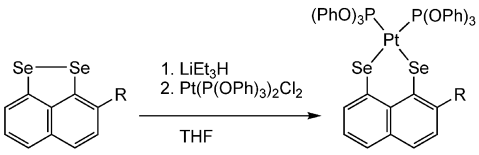

Scheme 2. Synthesis of **1** and **2**.

Complexes **1** and **2** have been fully characterized by elemental analysis, MS, IR, Raman, and ^{1}H, ^{13}C, ^{31}P, ^{77}Se, and ^{195}Pt NMR spectroscopy. We were unable to isolate bulk samples of complexes **3**–**5** and these complexes have been characterized by X-ray crystallography and multinuclear NMR spectroscopy.

The ^{31}P, ^{77}Se, and ^{195}Pt NMR spectroscopic data for **1**–**5** are given in Table 2 In its ^{31}P NMR spectrum, **1** displays a singlet at δ = 87 ppm, and both platinum ($J_{P,Pt}$ = 4711 Hz) and selenium ($J_{P\text{-}Se}$ = 28 Hz) satellites are visible. The ^{77}Se NMR contains a peak at δ = 140 ppm ($J_{Se\text{-}P}$ = 28 Hz) ($J_{Se\text{-}Pt}$ = 205 Hz). The ^{195}Pt NMR displays a triplet centered at –4711 ppm with selenium satellites visible ($J_{Pt,P}$ = 4711 Hz) ($J_{Pt\text{-}Se}$ = 205 Hz).

The ^{31}P NMR spectrum for **2** displays a typical [ABX]-pattern (A = P^{III}, X = Pt) indicative of direct coordination of two inequivalent phosphorus atoms to the platinum center. Both signals have platinum and selenium satellites; δ = 89 ($J_{P\text{-}P}$ = 68 Hz) ($J_{P,Pt}$ = 4686 Hz) ($J_{P\text{-}Se}$ = 19, 28); δ = 86 ($J_{P\text{-}P}$ = 68 Hz) ($J_{P,Pt}$ = 4669 Hz) ($J_{P\text{-}Se}$ = 35 Hz). The ^{77}Se NMR of **2** consists of two signals, each split by two inequivalent phosphorus atoms into a doublet of doublets with platinum satellites. The upfield peak at δ = 138 ppm is assigned to the ^{77}Se furthest from the *tert*-butyl arm by comparison with **1**. The ^{195}Pt NMR displays an apparent triplet

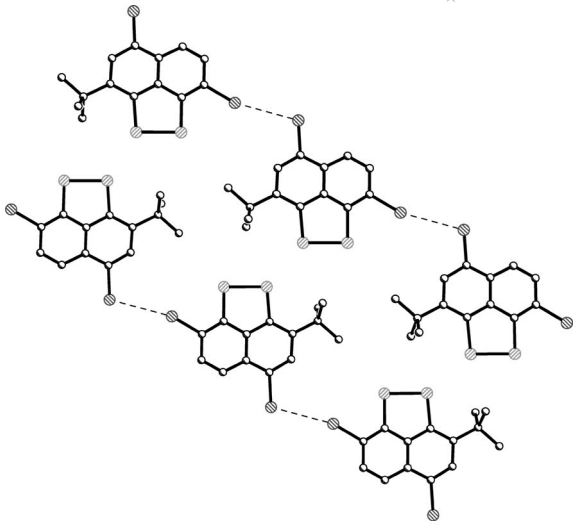

Figure 10. View of crystal packing in mt-Se_2naphBr_2 along the *b*-axis.

Table 2. NMR[a] data for complexes **1**–**5**.

	1	**2**[b]	**2**[c]	**3**	**4/5**
δ = ^{31}P [ppm]	87	89	86	85	84
J_{P-P} [Hz]		68	68		
$J_{P,Pt}$ [Hz]	4711	4686	4669	4685	4724
J_{P-Se} [Hz]	28	19, 28	35	21	28
δ = ^{77}Se	140 (t)	258 (dd)	138 (dd)	225 (t)	222 (t)
J_{Se-P} [Hz]	28	19, 35	7, 28	21	28
J_{Se-Pt} [Hz]	205	327	212	183	188
δ = ^{195}Pt	–4711 (t)	–4575 (dd)		–4570 (t)	–4075
$J_{Pt,P}$ [Hz]	4711	4979		4685	4729
J_{Pt-Se} [Hz]	205			183	

[a] All NMR samples were prepared from crystalline samples in $CDCl_3$. [b] In complex **2**, two signals result from the ^{77}Se atom present in one of two inequivalent positions, either the position closest to or furthest away from the substituted *tert*-butyl arm. At this time, based on comparisons to complex **1**, it is thought that the ^{77}Se peak at δ = 138 ppm corresponds to the ^{77}Se atom furthest from the *tert*-butyl substituent. [c] See footnote [b].

(doublet of doublets with similar coupling constants) centered at –4575 ppm ($J_{Pt,P} \approx 4680$ Hz).

The NMR spectroscopic data for **3** indicates the mononuclear complex [Pt(*dibenzSe*$_2$){P(OPh)$_3$}$_2$] is the predominant species in solution.[19] The ^{31}P NMR for **3** displays a typical [AX]-pattern relating to the direct coordination of two equivalent phosphorus atoms to the platinum center and selenium satellites are also observed; δ = 85 ($J_{P,Pt}$ = 4685 Hz) (J_{P-Se} = 21). The ^{77}Se NMR displays a triplet with platinum satellites at δ = 225 (J_{Se-P} = 21 Hz) (J_{Se-Pt} = 183 Hz). The ^{195}Pt NMR spectrum displays a triplet centered at –4570 ppm with selenium satellites visible ($J_{Pt,P}$ = 4685 Hz) (J_{Pt-Se} = 183 Hz). We were unable to separate **4** and **5** and the ^{31}P, ^{77}Se, and ^{195}Pt NMR spectra were measured using samples that contained crystalline material of at least some crystals of both complexes, as determined by X-ray studies. The NMR spectroscopic data, however, are indicative of the presence in solution of just compound **4**.

The ^{31}P NMR spectrum displays a typical [AAX]-pattern with a single signal at δ = 85 ppm with platinum satellites ($J_{P,Pt}$ = 4724 Hz). As in **3**, the ^{77}Se NMR spectrum of **4/5** exhibits a triplet with platinum satellites; δ = 222 (J_{Se-P} = 28 Hz) (J_{Se-Pt} = 188 Hz). The ^{195}Pt NMR spectrum displays a triplet centered at –4075 ppm ($J_{Pt,P}$ = 4729 Hz).

The X-ray crystal structures of **1**, **2**, and **4a** are shown in Figure 11, while Figure 12 shows **3** and **5**. The X-ray analyses show that in every complex, the platinum center lies in a distorted square-planar environment.

The differing molecular structures of **4** and **5** were quite unexpected. As described above, the ^{31}P NMR clearly suggest that only one species is present in the solution after synthesis and purification of the reaction mixture. Crystallization using pentane diffusion into a dichloromethane solution produced orange block crystals, which were characterized by X-ray crystallography, revealing the monomeric

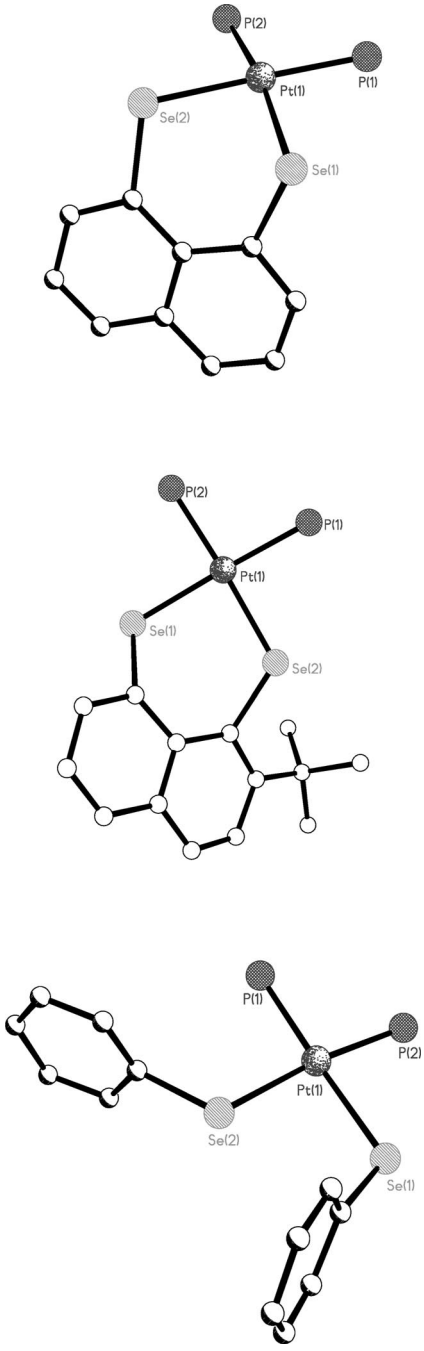

Figure 11. Molecular representations of the core atoms in **1** (top), **2** (middle), and one molecule of **4a** (bottom).

structure of **4**, however, this same solution also yielded crystals of binuclear **5**.

Complexes **1**, **2**, and **4** have strong similarities. Selected bond lengths and angles can be found in Table 3. Each of these complexes is monomeric, containing a four-coordinate Pt^{II} center having two –P(OPh)$_3$ ligands and two selenium ions from one or more of the selenium containing ligands. A comparison of bond lengths within this series of mononuclear complexes shows that all of these complexes have very similar Pt–P bond lengths ranging from 2.2232(13) Å to 2.2390(16) Å, with complex **2** having the

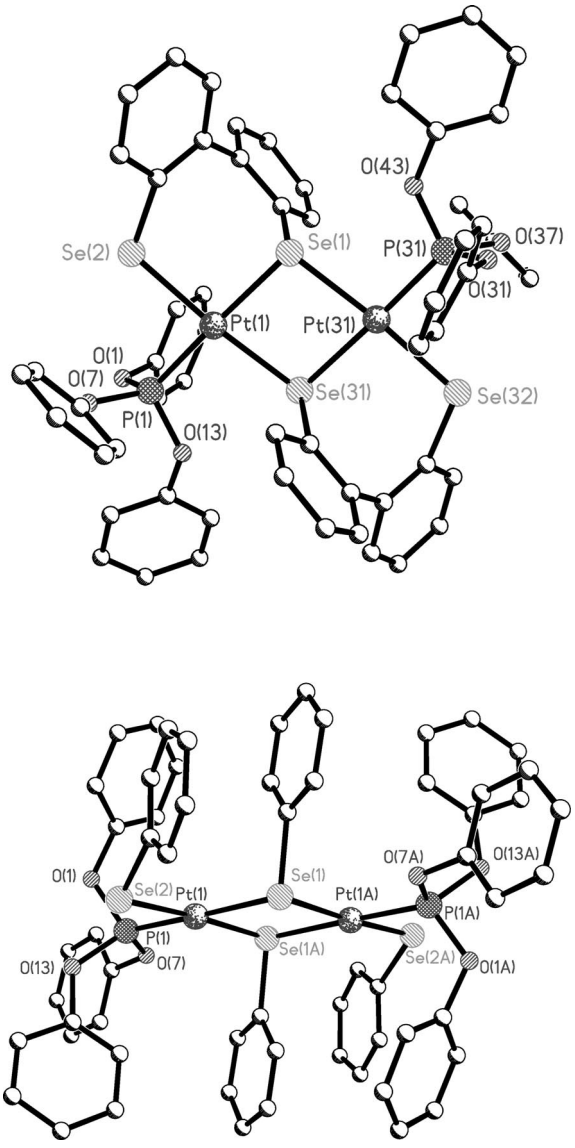

Figure 12. Molecular representations of **3** (top) and **5** (bottom).

shortest Pt–P bond length. The Pt–Se bond lengths have a larger difference. The Pt–Se bond lengths are longest in **4/4a** ranging from 2.481(2) Å to 2.463(2) Å, slightly shorter in **1** at 2.4600(7) Å and 2.4527(7) Å, and yet shorter in **2** at 2.4356(5) Å and 2.4256(5) Å. The short Pt–Se distances in **2** are possibly an effect of the electron donating *tert*-butyl arm on the naphthalene ring. It is noticeable on going from **1** to **2** the six membered $PtSe_2C_3$ ring changes substantially. In **1** the ring is essentially a boat conformation with a hinge at the Se···Se vector whilst in **2** the ring is a twisted chair conformation this difference presumably arises as a consequence of the sterically demanding *tert*-butyl group in **2**.

The Se(1)–Pt(1)–Se(2) bond angles increase from 85.55(2)° in **1**, to 87.47(7)° in **4** to 89.43(8)° in **4a**, and finally to 89.885(17)° in **2**. It is interesting that the only difference between **1** (the smallest angle) and **2** (the largest angle) is the substitution of the *tert*-butyl substituent on the naphthalene ring. The steric bulk of the *tert*-butyl group

Table 3. Selected interatomic distances [Å] and angles [°] for **1**, **2**, and **4** (**4**[1] is the second independent molecule of **4**).

	1	**2**	**4**	**4**[1]
Pt(1)–Se(1)	2.4600(7)	2.4356(5)	2.474(2)	2.481(2)
Pt(1)–Se(2)	2.4527(7)	2.4256(5)	2.463(2)	2.481(2)
Pt(1)–P(1)	2.2390(16)	2.2232(13)	2.229(5)	2.235(5)
Pt(1)–P(2)	2.2324(14)	2.2385(14)	2.224(4)	2.235(5)
Se(1)–C(1)	1.921(6)	1.914(5)	1.85(2)	1.87(2)
Se(2)–C	1.924(6)	1.930(4)	1.94(2)	
Se(1)–Pt(1)–Se(2)	85.55(2)	89.885(17)	87.47(7)	89.43(8)
Se(1)–Pt(1)–P(1)	91.19(4)	86.94(3)	177.85(13)	171.09(14)
Se(2)–Pt(1)–P(2)	88.80(4)	88.02(4)	173.70(14)	171.09(14)
P(1)–Pt(1)–P(2)	94.67(6)	95.29(4)	92.35(18)	99.3(2)
Se(1)–Pt(1)–P(2)	169.82(5)	176.93(3)	86.50(13)	86.11(15)
Se(2)–Pt(1)–P(1)	176.33(4)	175.08(3)	93.73(13)	86.11(15)
Pt(1)–Se(1)–C(1)	100.17(17)	107.59(13)	110.3(6)	105.0(6)
Pt(1)–Se(2)–C	107.63(18)	116.77(15)	112.8(5)	105.0(6)

pushes the selenium atom nearest to it out of the plane of the naphthalene ring, rendering the Se–Pt–Se bond angle larger than in **1**, where the selenium atoms may be constrained by a need to stay in the plane of the rings to participate in π-resonance. However, the size of the Se(1)–Pt(1)–Se(2) bond angle in **4** falls in the middle of the series of complexes, despite not being restricted by the backbone, as in **1** and **2**. The similarity of the bond angle (only ca. 4° difference) amongst the complexes is likely not coincidental, even if the ligands have no strong geometric preferences, the geometry of the complex is still limited by the tendency of Pt^{II} to be square planar.

Compared to **4** in the Se–Pt–Se angles, the *cis*-bond angles Se–Pt–P in the three complexes are universally similar. The Se(1)–Pt(1)–P(2) bond angle in **4** is 86.50(13)° and the Se(2)–Pt(1)–P(1) bond angle is 93.73(13)° with the Se(1)–Pt(1)–P(1) bond angle being 91.19(4)° and the Se(2)–Pt(1)–P(2) bond angle being 88.80(4)°. The bond angle differences in **2** are similar to the other two complexes, with the Se(1)–Pt(1)–P(1) bond angle being 86.94(3)° and the Se(2)–Pt(1)–P(2) bond angle being 88.02(4)°. The two *trans* Se–Pt–P bond angles of the three complexes likewise differ from each other by only a few degrees. The difference between the two angles is 7.5° in **1**, 4.2° in **4** and 1.8° in **2**.

The smallest of the *trans* Se–Pt–P bond angles occurs in **1**, with an angle of 169.82(5)°. Other than a bond angle of 173.40(14)° in **4**, all the other *trans* bond angles in all three complexes are very close to 176°. Like all the other angles, the P(1)–Pt(1)–P(2) bond angles of **1**, **2**, and **4** are very similar, except in **4b**, where it is the largest by 4° at 99.3(2)°. Somewhat strangely, the steric strain presented by the *tert*-butyl group in **2** and the greater degree of freedom allowed by the lack of a constraining background in **4** do not seem to cause much variation in the structure around the metal center. The metal center appears to be dictating the geometry and forcing the ligands to arrange themselves so that the complex has as close to a square planar motif it can.

Complexes **3** and **5** are different from the three just discussed, in that they each crystallize as a dinuclear complex with two four-coordinate Pt^{II} metal centers in a diamond

core motif. Each Pt^{II} ion in both complexes is coordinated by three selenium ions and one $-P(OPh)_3$ ligand. A list of selected bond lengths and angles for **3** and **5** are shown in Tables 4 and 5. The difference between the two coordination spheres is that **3** has dianionic bis-selenium ligands based on the biphenyl backbone, while the platinum centers in **5** are ligated by individual *SePh* ligands. One of the selenium atoms on the biphenyl in **3** is in a bridging position, which forces the ligand to twist and strain in order for the platinum to coordinate the other selenium atom. In **5**, the bridging and terminal positions are occupied by the *SePh* ligands instead.

Table 4. Selected interatomic distances [Å] and angles [°] for complex **3**.

Pt(1)–P(1)	2.202(2)	Pt(31)–P(31)	2.200(2)
Pt(1)–Se(2)	2.4370(10)	Pt(31)–Se(32)	2.4449(11)
Pt(1)–Se(31)	2.4582(10)	Pt(31)–Se(31)	2.4544(10)
Pt(1)–Se(1)	2.4569(10)	Pt(31)–Se(1)	2.4628(10)
Se(1)–C(19)	1.928(9)		
Se(31)–C(49)	1.944(10)		
Se(32)–C(56)	1.960(9)		
Se(2)–C(26)	1.922(10)		
P(1)–Pt(1)–Se(2)	88.50(7)	P(31)–Pt(31)–Se(32)	88.72(7)
P(1)–Pt(1)–Se(31)	93.86(7)	P(31)–Pt(31)–Se(1)	94.00(7)
Se(2)–Pt(1)–Se(1)	93.64(3)	Se(32)–Pt(31)–Se(31)	93.44(4)
Se(31)–Pt(1)–Se(1)	83.89(3)	Se(31)–Pt(31)–Se(1)	83.85(3)
Se(2)–Pt(1)–Se(31)	173.11(4)	Se(32)–Pt(31)–Se(1)	172.28(4)
P(1)–Pt(1)–Se(1)	177.60(7)	P(31)–Pt(31)–Se(31)	177.84(7)
C(19)–Se(1)–Pt(1)	93.9(3)	C(49)–Se(31)–Pt(31)	93.2(3)
C(19)–Se(1)–Pt(31)	106.5(3)	C(49)–Se(31)–Pt(1)	107.1(3)
Pt(1)–Se(1)–Pt(31)	96.04(3)	Pt(31)–Se(31)–Pt(1)	96.22(3)
C(26)–Se(2)–Pt(1)	110.1(3)	C(56)–Se(32)–Pt(31)	110.6(3)

Table 5. Selected interatomic distances [Å] and angles [°] for **5**.

Pt(1)–P(1)	2.186(2)	Pt(31)–P(31)	2.193(2)
Pt(1)–Se(2)	2.4493(9)	Pt(31)–Se(32)	2.4445(8)
Pt(1)–Se(1A)	2.4697(9)	Pt(31)–Se(3A)	2.4632(8)
Pt(1)–Se(1)	2.4771(8)	Pt(31)–Se(31)	2.4763(8)
Se(1)–Pt(1A)	2.4697(9)	Se(31)–Pt(3A)	2.4632(8)
Se(1)–C(19)	1.927(7)	Se(31)–C(49)	1.931(7)
Se(2)–C(25)	1.932(8)	Se(32)–C(55)	1.925(8)
P(1)–Pt(1)–Se(2)	85.83(6)	P(31)–Pt(31)–Se(32)	84.01(5)
P(1)–Pt(1)–Se(1A)	95.66(6)	P(31)–Pt(31)–Se(3A)	96.90(5)
Se(2)–Pt(1)–Se(1)	94.71(3)	Se(3A)–Pt(31)–Se(31)	84.07(3)
Se(1A)–Pt(1)–Se(1)	83.89(3)	Se(32)–Pt(31)–Se(31)	94.99(3)
Se(2)–Pt(1)–Se(1A)	175.74(3)	Se(32)–Pt(31)–Se(3A)	176.46(3)
P(1)–Pt(1)–Se(1)	178.57(5)	P(31)–Pt(31)–Se(31)	178.86(6)
C(19)–Se(1)–Pt(1A)	98.9(2)	C(49)–Se(31)–Pt(3A)	100.5(2)
C(19)–Se(1)–Pt(1)	104.2(2)	C(49)–Se(31)–Pt(31)	103.7(2)
Pt(1A)–Se(1)–Pt(1)	96.11(3)	Pt(3A)–Se(31)–Pt(31)	95.93(3)
C(25)–Se(2)–Pt(1)	106.6(2)	C(55)–Se(32)–Pt(31)	106.3(2)

Rather unsurprisingly, given their similar coordination spheres, the bond lengths in **3** and **5** are very similar throughout the complexes (Table 4, Table 5). The Pt–P bond lengths are similar at ca. 2.20 Å in **3** and ca. 2.19 Å in **5**. The Pt–Se bonds in both complexes differ depending on whether they are coordinated in a terminal or bridging fashion, but are again markedly similar between the two complexes. In **3**, the terminal Pt–Se bond lengths are ≈ 2.44 Å, whereas the bridging bond lengths are about 2.46 Å. In **5**, the terminal Pt–Se bond lengths are ca. 2.45 Å, and the bridging bond lengths are ca. 2.47 Å.

Like the bond lengths, the bond angles in **3** and **5** are very similar. Complex **3** has two obtuse angles and two acute angles around the platinum centers, which form a flattened X with a platinum atom in the center. The Se–Pt–Se bond angle of the diamond core is 83.89(3)°, and the bond *trans* to this, across the platinum center, is 88.50(7)°. The other two angles around the platinum center are ca. 94°. The Pt–Se–Pt bond bridging the diamond core is 96.04(3)°.

The bond angles in **5** track very closely to those in **3**. The Se–Pt–Se bond angle of the diamond core is 83.89(3)° and *trans* to this, the angle is 85.83(6)°. The other two angles around the platinum center are 94.71(3)° and 95.66(6)°. The bridging Pt–Se–Pt angles are both almost exactly 96°. From this data, it seems as though the visibly twisted biphenyl-based diselenium ligand is not responsible for the distortion of the geometry around the metal center in **3**, since the *SePh* ligands in **5** end up giving the complex an extremely similar set of bond lengths and angles without the ligand imposing a geometric restriction.

Experimental Section

General: All synthetic procedures were performed under nitrogen using standard Schlenk techniques unless otherwise stated, reagents were obtained from commercial sources and used as received. Dry solvents were collected from an MBraun solvent system. ^{1}H, ^{13}C, ^{31}P, and ^{77}Se spectra were recorded on a Jeol DELTA GSX270 spectrometer. ^{195}Pt spectra were obtained on a Bruker AVII400. Chemical shifts are reported in ppm and coupling constants (*J*) are given in Hz. IR (KBr pellet) and Raman spectra (powder sample) were obtained on a Perkin–Elmer system 2000 Fourier Transform spectrometer. Elemental analysis was performed by the University of St. Andrews, School of Chemistry Service. Positive-ion FAB mass spectra were performed by the EPSRC National Mass Spectrometry Service, Swansea. Precious metals were provided by Ceimig Ltd.

Synthetic Remarks: The compound *cis*-$[Pt\{P(OPh)_3\}_2Cl_2]$ was prepared by adding two equivalents of $P(OPh)_3$ to *cis*-$[PtCl_2(cod)]$ (cod = 1,5-cyclooctadiene) in dichloromethane at room temperature instead of by the procedure reported by Sabounchei et al.[20]

Synthesis of Naphtho[1,8-*c*,*d*][1,2]diselenole (Se_2naph): Crystalline naphthalene (6.10 g, 47.6 mmol) was added to a 500 mL round bottom Schlenk flask. The flask was evacuated and purged with nitrogen. Butyllithium (BuLi) (46.8 mL of 2.5 M in THF, 117 mmol) was added dropwise via syringe with stirring, followed by the slow addition of TMEDA (17.7 mL, 117 mmol). Upon addition, the flask became slightly warm and a white precipitate (pcc) formed. The pcc dissolved as the solution yellowed and then became increasingly darker until it was dark reddish in color. A reflux condenser was added to the flask, which was then warmed to ca. 70 °C for two hours. The mixture was allowed to cool to room temperature,

at which time the reflux condenser was replaced by a septum. The mixture was then cooled to –70 °C using a dry ice/acetone bath. Tetrahydrofuran (THF) (ca. 150 mL) was added dropwise via syringe. Selenium powder (11.1 g, 141 mmol) was then added at once. The reaction mixture was allowed to slowly warm to room temperature and was stirred overnight under nitrogen.

Caution! As the mixture warms to room temperature, the flask becomes slightly pressurized. Make sure the stopper is clipped and the flask is opened to nitrogen.

The next day, the flask was opened and the mixture was poured into a 2 separating funnel where ca. 500 mL of distilled water and ca. 300 mL of hexane was then added. It was difficult to see the separation line, but as the water layer was removed the line became more evident. The hexane layer, a clear purple solution, was collected. Silica gel was added to the organic layer and the solvent was evaporated. The silica gel/product was placed on top of a silica column and the product was eluted with hexane. The purple band was collected and the solvent evaporated. The purple solid was dissolved in a minimal amount of dichloromethane. The solution was then layered with hexane and placed in the freezer for recrystallization; yield 3.544 g, 26%. ^{1}H and ^{77}Se NMR matched those of the previous reported samples.[1]

Synthesis of 2,7-Di-*tert*-butylnaphtho[1,8-*c*,*d*][1,2]diselenole (dt-Se_2naph) and 2-*tert*-butylnaphtho[1,8-*c*,*d*][1,2]diselenole (mt-Se_2naph): 2,7-Di-*tert*-butylnaphtho[1,8-*c*,*d*][1,2]diselenole (dt-Se_2naph) and 2-*tert*-butylnaphtho[1,8-*c*,*d*][1,2]diselenole (mt-Se_2naph) were prepared by methods reported for the thiol analogues.[15,16] Se_2naph (0.38 g, 1.3 mmol), *tert*-butyl chloride (0.43 mL, 3.9 mmol), and CH_3NO_2 (ca. 7 mL), were added to a 100 mL round bottom Schlenk flask. The reaction was heated with stirring to about 80 °C and $AlCl_3$ (36 mg, 0.27 mmol) was added. The mixture continued to heat at about 80 °C for one hour. After the reaction cooled to room temperature, distilled water was added, which then was extracted with dichloromethane. The organic layer was removed, dried with $MgSO_4$, filtered, and the solvent was evaporated. These compounds were purified by column chromatography on silica gel elution using hexane, with mt-Se_2naph eluting first, then dt-Se_2naph, followed by starting material. dt-Se_2naph was crystallized by slow evaporation of a pentane solution to give orange blocks (17 mg, 3%). mt-Se_2naph is a dark red oil (104 mg, 23%), and finally 81 mg (21%) of the starting material was recovered.

mt-Se_2naph: ^{1}H NMR ($CDCl_3$): δ = 7.52–7.17 (m, 5 H), 1.53 (s, 9 H) ppm. ^{77}Se NMR ($CDCl_3$): δ = 414 (s), 414 (d, $J_{Se\text{-}Se}$ = 345 Hz), 360 (s), 360 (d, $J_{Se\text{-}Se}$ = 345 Hz) ppm. ^{13}C NMR ($CDCl_3$): δ = 144.3, 139.5, 138.8, 138.3, 136.5, 126.8, 125.8, 124.8, 123.3, 122.0, 36.5, 29.2 ppm. MS (TOF MS CI):*m*/*z* = 339 [^{78}Se, ^{80}Se], 341 [^{80}Se].

dt-Se_2naph: ^{1}HNMR ($CDCl_3$): δ = 7.52–7.44 (m, $J_{H,H}$ = 8, 21 Hz, 4 H), 1.56 (s, 18 H) ppm. ^{77}SeNMR ($CDCl_3$): δ = 353 (s) ppm. ^{13}CNMR ($CDCl_3$): δ = 144.05, 140.37, 136.99, 134.98, 125.82, 124.37, 36.66, 29.10 ppm. MS (TOF MS CI): *m*/*z* = 396 [^{78}Se, ^{80}Se], 398 [^{80}Se].

Synthesis of 4,7-Dibromo-2-*tert*-butylnaphtho[1,8-*c*,*d*][1,2]diselenole (Se_2naphBr_2): A solution of 2-*tert*-butylnaphtho[1,8-*c*,*d*][1,2]diselenole (mt-Se_2naph) (0.11 g, 0.33 mmol) in dichloromethane (10 mL) was cooled to 0 °C and slowly treated with bromine (0.11 g, 0.034 mL, 0.66 mmol). An analytically pure sample was obtained by crystallisation from diffusion of pentane into a dichloromethane solution of the product (0.1 g, 74%). IR (KBr tablet): $\tilde{\nu}_{max}$ = 3424 (br. s), 3069 (w), 2955 (s), 2854 (w), 1584 (w), 1568 (w), 1514 (w), 1482 (s), 1466 (vs), 1392 (s), 1361 (s), 1282 (s), 1218 (s), 1186 (w), 1147 (s), 1116 (vs), 996 (vs), 913 (s), 881 (s), 860 (w), 820 (s), 799 (s), 741 (s), 663 (w), 558 (w), 509 (w), 485 (w), 468 (w), 381 (w) cm^{-1}. ^{1}HNMR ($CDCl_3$): δ = 7.77–7.64 (m, 2 H, 3,5-H), 7.53–7.40 (m, 1 H, 6-H), 1.52 [s, 9 H, -C(CH_3)$_3$] ppm. ^{13}C NMR ($CDCl_3$): δ = 134.5 (s), 133.6 (s), 132.9 (s), 131.4 (s), 131.2 (s), 130.6 (s), 130.2 (s), 130.1 (s), 124.9 (s), 124.1 (s), 29.8 (s), 28.7 (s) ppm. ^{77}SeNMR ($CDCl_3$): δ = 454, 374 ppm. MS (TOF MS EI$^+$): *m*/*z* (%) =497.98 (100) [M$^+$].

Synthesis for [Pt(L){P(OPh)$_3$}$_2$], L = Se_2naph (1) and mt-Se_2naph (2): In a Schlenk tube, ca. 10 mL of dry THF was added to 1 mol-equiv. of **L**, the resulting purple solution was stirred for 10 min and then, 2 mol-equiv. of a 1 M solution of $LiBEt_3H$ in THF was added dropwise via syringe. Upon addition, the purple solution turned bright yellow and gas evolution was observed. This solution was stirred ca. 15 min and [Pt{P(OPh)$_3$}$_2$Cl$_2$] was added. The solution turned orange in color and was stirred 12 h, after which ca. 1 g of silica gel was added and the solvent was evaporated under vacuum. The flask containing the orange solid was opened to the air and the solid was placed on top of a short hexane-packed silica gel column. The column was eluted with hexane to remove any unreacted starting material and then washed with CH_2Cl_2. The CH_2Cl_2 band was collected and the solvent was removed under vacuum. Orange crystals were obtained for **1** (97 mg, 53%) and **2** (109 mg, 50%) after recrystallization from CH_2Cl_2 by pentane diffusion.

[Pt(*Se_2naph*){P(OPh)$_3$}$_2$] (1): Se_2naph (47 mg, 165 mmol), 0.33 mL of 1 M soln of $LiBEt_3H$ in THF, and [Pt{P(OPh)$_3$}$_2$Cl$_2$] (147 mg, 165 mmol). $C_{46}H_{36}O_6P_2PtSe_2{\cdot}CH_2Cl_2$: calcd. C 47.60, H 3.23; found C 47.79, H 3.10. FAB$^+$ MS: *m*/*z* = 1100 [M$^+$]. IR (KBr): $\tilde{\nu}_{max}$ = 1587, 1486, 1182, 1159, 918, 778, 757, 687, 596, 496 cm^{-1}. Raman: $\tilde{\nu}$ = 30720, 1591, 1538, 1333, 1007, 851, 733, 530, 200 cm^{-1}. All NMR samples were prepared from crystalline samples in $CDCl_3$. ^{1}H NMR: δ = 7.6 (d, $J_{H,H}$ = 7 Hz), 7.5 (d, $J_{H,H}$ = 7 Hz), 7.2–6.9 (m), 6.9 (t, $J_{H,H}$ = 7 Hz) ppm. ^{13}C NMR: δ = 150.9, 136.3, 135.1, 129.8, 126.9, 125.2, 124.7, 120.9 ppm. ^{31}P NMR: δ = 87 ppm ($J_{P,Pt}$ = 4711 Hz) ($J_{P\text{-}Se}$ = 28 Hz). ^{77}Se NMR: δ = 140 ppm (t, $J_{Se\text{-}P}$ = 28 Hz) ($J_{Se\text{-}Pt}$ = 205 Hz). ^{195}Pt NMR: δ = –4711 ppm (t, $J_{Pt,P}$ = 4711 Hz) ($J_{Pt\text{-}Se}$ = 205 Hz).

[Pt(*mt-Se_2naph*){P(OPh)$_3$}$_2$] (2): mt-Se_2naph (64 mg, 187 mmol), 0.37 mL of 1 M soln of $LiBEt_3H$ in THF, and [Pt{P(OPh)$_3$}$_2$Cl$_2$] (166 mg, 187 mmol). $C_{50}H_{44}O_6P_2PtSe_2{\cdot}0.5CH_2Cl_2$:: calcd. C 50.50, H 3.78; found C 50.51, H 3.49. FAB$^+$ MS: *m*/*z* = 1156 [M$^+$]. IR (KBr): $\tilde{\nu}_{max}$ = 1588, 1488, 1186, 1160, 922, 776, 756, 686, 595, 497 cm^{-1}. Raman: $\tilde{\nu}$ = 3066, 1595, 1586, 1515, 1340, 1007, 857, 733, 185 cm^{-1}. All NMR samples were prepared from crystalline samples in $CDCl_3$. ^{1}H NMR: δ = 7.4–7.0 (m), 6.9 (t, $J_{H,H}$ = 7 Hz)., 1.7 (s) ppm. ^{13}C NMR: δ = 151.0, 150.9, 147.0, 142.5, 132.9, 132.1, 131.9, 129.7, 129.6, 126.5, 125.5, 125.2, 125.0, 123.9, 123.2, 121.0, 120.9, 120.7, 120.6, 38.2, 31.6 ppm. ^{31}P NMR: δ = 89 ppm (d, $J_{P\text{-}P}$ = 68 Hz), ($J_{P,Pt}$ = 4686 Hz) ($J_{P\text{-}Se}$ = 19, 28) 86 ppm (d, $J_{P\ P}$ = 68 Hz), ($J_{P,Pt}$ = 4669 Hz) ($J_{P\ Se}$ = 35). ^{77}Se NMR: δ = 258 ppm (dd, $J_{Se\text{-}P}$ = 19, 35 Hz) ($J_{Se\text{-}Pt}$ = 329 Hz), 138 ppm (dd, $J_{Se\text{-}P}$ = 7, 28 Hz) ($J_{Se\text{-}Pt}$ = 212 Hz). ^{195}Pt NMR: δ = –4575 ppm (observed is apparent triplet $J_{Pt,P} \approx$ 4680 Hz).

Synthesis of [Pt$_2$(*dibenzSe_2*)$_2${P(OPh)$_3$}$_2$] (3): In a Schlenk tube, ca. 10 mL of dry THF was added to 1 mol-equiv. of dibenzSe_2, the resulting pale orange solution was stirred for 10 min and then 2 mol-equiv. of a 1 M solution of $LiBEt_3H$ in THF was added dropwise via syringe. Upon addition, the solution turned very pale yellow, then clear with gas evolution. This solution was stirred ca. 15 min and [Pt{P(OPh)$_3$}$_2$Cl$_2$] was added. The solution turned bright yellow in color and was stirred 12 h, after which time ca. 1 g of silica gel was added and the solvent was evaporated under vac-

uum. The flask containing the yellow solid was opened to the air and the solid was placed on top of a short hexane-packed silica gel column. The column was eluted with hexane to remove any unreacted starting material and then washed with 2:1 CH_2Cl_2/hexane. The resulting bright yellow band was collected and the solvent was removed under vacuum. X-ray quality crystals were obtained for **3** after recrystallization from CH_2Cl_2 by pentane diffusion. FAB^+ MS: *m/z* 1631 [M^+] (matches theoretical isotope profile for **3**). IR (KBr): $\tilde{\nu}_{max}$ = 1588, 1486, 1184, 1160, 1025, 922, 765, 687, 595, 491 cm^{-1}. Raman IR: $\tilde{\nu}$ = 3066, 1589, 1030, 1008 cm^{-1}. NMR samples were prepared from crystalline samples in $CDCl_3$. ^{31}P NMR: δ = 85 ppm ($J_{P,Pt}$ = 4685 Hz) ($J_{P\text{-}Se}$ = 21). ^{77}Se NMR: δ = 225 ppm (t, $J_{P\text{-}Se}$ = 21) ($J_{Pt\text{-}Se}$ = 183 Hz). ^{195}Pt NMR: δ = –4570 ppm (t, $J_{Pt,P}$ = 4685 Hz) ($J_{Pt\text{-}Se}$ = 183 Hz). The NMR spectroscopic data seem to suggest that the predominant species in solution is [Pt(dibenzSe$_2$){P(OPh)$_3$}$_2$].

Synthesis of *cis*-[Pt(*SePh*)$_2${P(OPh)$_3$}$_2$] (4) and [Pt$_2$(SePh)$_4${P(OPh)$_3$}$_2$] (5): In a Schlenk tube, ca. 10 mL of dry THF was added to 1 mol-equiv. of Se_2Ph_2, the resulting yellow solution was stirred for 10 min and then 2 mol-equiv. of a 1 M solution of $LiBEt_3H$ in THF was added dropwise via syringe. Upon addition, the solution turned pale yellow with gas evolution. This solution was stirred ca. 15 min and [Pt{P(OPh)$_3$}$_2$Cl$_2$] was added. The solution turned bright orange in color and was stirred 12 h, after which time ca. 1 g of silica gel was added and the solvent was evaporated. The flask containing the orange solid was opened to the air and the solid was placed on a small hexane silica gel column. The column was eluted with hexane to remove any unreacted starting material and then washed with 2:1 CH_2Cl_2/hexane. This orange band was collected and the solvent was removed under vacuum. Complexes **4** and **5** co-crystallized out of the same CH_2Cl_2 solution by pentane diffusion. Complex **4** is deep orange in color, almost red, whereas **5** is bright yellow. All data was obtained from crystalline solid that contained both **4** and **5**. $C_{48}H_{40}O_6P_2PtSe_2$ (**4**) (1127.80): calcd. C 51.12, H 3.57 and for $C_{60}H_{50}O_6P_2Pt_2Se_4$ (**5**) (1635.02): calcd. C 44.08, H 3.08; found C 44.62, H 2.81. FAB^+ MS: *m/z* 1635 [M^+] (matches theoretical isotope profile for **5**, but there are higher molecular ion peaks in the sample). IR (KBr): $\tilde{\nu}_{max}$ = 1587, 1485, 1183, 1156, 919, 784, 686, 601, 488 cm^{-1}. Raman IR: $\tilde{\nu}$ = 3063, 1597, 1576, 1220, 1169, 1071, 1001, 226, 178 cm^{-1}. NMR samples were prepared in $CDCl_3$. ^{31}P NMR: δ = 84 ppm. ($J_{P,Pt}$ = 4724 Hz) ($J_{P\text{-}Se}$ = 28 Hz). ^{77}Se NMR: δ = 222 ppm (t, $J_{P\text{-}Se}$ = 28 Hz) ($J_{Se\text{-}Pt}$ = 188 Hz). ^{195}Pt NMR: δ = –4075 ppm (t, $J_{Pt,P}$ = 4729 Hz). NMR spectroscopic data seem to suggest that the mononuclear species **4** exists in solution, rather than the dinuclear species **5**.

Table 6. Crystallographic data for compounds dt-Se_2naph, mt-Se_2naphBr_2 and **1**–**5**.

	dt-Se_2naph	mt-Se_2naphBr_2	1	2	3	4	5
Empirical formula	$C_{18}H_{22}Se_2$	$C_{14}H_{14}Br_2Se_2$	$C_{46}H_{36}O_6Se_2P_2Pt$	$PtC_{51}H_{46}O_6P_2Se_2Cl_2$	$C_{62}H_{50}Cl_4O_6P_2Pt_2Se_4$	$C_{146}H_{124}O_{18}P_6Pt_3Se_6Cl_4$	$C_{60}H_{50}O_6P_2Pt_2Se_4$
Formula weight	396.29	499.99	1099.74	1240.78	1800.78	3553.26	1634.96
Temperature [°C]	–148(1)	–148(1)	–148(1)	–148(1)	–180(1)	–148(1)	–180(1)
Crystal colour, habit	orange, block	red, prism	orange, block	yellow, platelet	yellow, prism	orange, block	yellow, prism
Crystal dimensions [mm^3]	0.55×0.40×0.30	0.09×0.06×0.06	0.22×0.15×0.07	0.41×0.14×0.10	0.20×0.20×0.20	0.52×0.10×0.06	0.10×0.03×0.03
Crystal system	orthorhombic	monoclinic	orthorhombic	monoclinic	monoclinic	monoclinic	triclinic
Lattice parameters	*a* = 11.333(11) Å	*a* = 9.638(7) Å	*a* = 13.3431(5) Å	*a* = 17.1347(5) Å	*a* = 12.0039(15) Å	*a* = 61.179(3) Å	*a* = 10.1847(12) Å
	b = 12.079(11) Å	*b* = 7.112(5) Å	*b* = 13.5580(5) Å	*b* = 26.5360(8) Å	*b* = 20.430(2) Å	*b* = 11.9162(4) Å	*b* = 13.7001(16) Å
	c = 12.029(11) Å	*c* = 10.499(8) Å	*c* = 22.8535(8) Å	*c* = 11.0032(3) Å	*c* = 25.009(3) Å	*c* = 18.9059(9) Å	*c* = 20.338(2) Å
	–	–	–	–	–	–	*α* = 83.840(7)°
	β = 90°	*β* = 94.263(15)°	*β* = 90°	*β* = 102.4922(8)°	*β* = 99.836(3)°	*β* = 98.6466(18)°	*β* = 82.868(7)°
	–	–	–	–	–	–	*γ* = 85.896(8)°
Volume [$Å^3$]	1647(3)	717.6(8)	4134.3(3)	4884.6(2)	6043.1(13)	13626.1(11)	2794.7(6)
Space group	*Pcca*	*P*2$_1$/*m*	*P*2$_1$2$_1$2$_1$	*Cc*	*Cc*	*C*2/*c*	*P*$\bar{1}$
Z value	4	2	4	4	4	4	2
$D_{calcd.}$ [g/cm^3]	1.598	2.314	1.767	1.687	1.979	1.732	1.943
F(000)	792	472	2144	2440	3440	6960	1560
m(Mo*Ka*) [cm^{-1}]	44.807	107.166	52.68	45.75	73.15	48.776	77.13
Number of reflections measured	13383	4132	43187	25442	19245	52775	18111
R_{int}	0.032	0.039	0.095	0.041	0.0453	0.329	0.047
Min.–max. transmissions	0.130–0.261	0.373–0.526	0.398–0.692	0.304–0.633	0.7102–1.0000	0.383–0.746	0.6118–1.0000
Independent reflections	1508	1362	9468	11089	8754	11981	9897
Observed reflection (no. variables)	1314 (94)	1267 (115)	8094 (515)	9956 (578)	7937 (722)	7175 (826)	7534 (688)
Reflection/parameter ratio	16.04	11.84	18.38	19.19	12.12	14.5	14.39
Residuals: R_1 [$I > 2.00s(I)$]	0.0385	0.0452	0.048	0.0345	0.0362	0.125	0.0453
Residuals: *R* (all reflections)	0.0444	0.0499	0.0629	0.042	0.0414	0.1953	0.067
Residuals: wR_2 (all reflections)	0.1011	0.1072	0.061	0.0543	0.0705	0.3989	0.0726
Goodness-of-fit indicator	1.093	1.181	1.051	0.987	0.874	1.145	0.975
Flack parameter	–	–	–0.006(5)	0.001(3)	–0.005(7)	–	–
Max. peak in final diff. map [$e/Å^3$]	0.83	0.66	2.59	1.54	1.744	6.56	1.807
Min. peak in final diff. map [$e/Å^3$]	–0.55	–0.99	–1.02	–0.70	–1.424	–10.18	–1.542

X-ray Crystallography: Crystal structure data for **1**, **2**, dt-Se_2naph and mt-Se_2naphBr_2 were collected using the St. Andrews Robotic Rigaku Saturn CCD diffractometer using Mo-K_α radiation (graphite monochromator optic, λ = 0.71073 Å), **4** was determined by using a Rigaku SCX-Mini whilst **3** and **5** were determined by using a Rigaku MM007 rotating anode and Mercury CCD. All data were corrected for absorption. The structure was solved by direct methods and refined by full-matrix least-squares methods on F^2 values of all data. Refinements were performed using SHELXTL (version 6.1, Bruker-AXS, Madison WI, USA, 2001). The experimental details including the results of the refinement are given in Table 6.

CCDC-759117 (for **1**), -759118 (for **2**), -759119 (for **3**), -759120 (for **4**), -759121 (for **5**), -759122 (for dt-Se_2naph), -759123 (for mt-Se_2naphBr_2) contain the supplementary crystallographic data for this paper. These data can be obtained free of charge from The Cambridge Crystallographic Data Centre via www.ccdc.cam.ac.uk/data_request/cif.

[1] J. Meinwald, D. Dauplaise, F. Wudl, J. J. Hauser, *J. Am. Chem. Soc.* **1977**, *99*, 255–257.

[2] K. Yui, Y. Aso, T. Otsubo, F. Ogura, *Bull. Chem. Soc. Jpn.* **1988**, *61*, 953–959.

[3] J. L. Kice, Y. Kang, M. B. Manek, *J. Org. Chem.* **1988**, *53*, 2435–2439.

[4] G. C. Hampson, A. Weissberger, *J. Chem. Soc.* **1936**, 393–398.

[5] S. Vyskocil, L. Meca, I. Tislerova, I. Cisarova, M. Polasek, S. R. Harutyunyan, Y. N. Belokon, M. J. Stead Russel, L. Farrugia, S. C. Lockhart, W. L. Mitchell, P. Kocovsky, *Chem. Eur. J.* **2002**, *8*, 4633–4648.

[6] A. J. Ashe III, J. W. Kampf, P. M. Savla, *Heteroat. Chem.* **1994**, *5*, 113–119.

[7] S. M. Aucott, H. L. Milton, S. D. Robertson, A. M. Z. Slawin, J. D. Woollins, *Heteroat. Chem.* **2004**, *15*, 530–542.

[8] J. D. Lee, M. W. R. Bryant, *Acta Crystallogr.* **1969**, *25*, 2094–2101.

[9] M. R. Bryce, A. Chesney, A. K. Lay, A. S. Batsanov, J. A. K. Howard, *J. Chem. Soc. Perkin Trans. 1* **1996**, 2451–2459.

[10] S. M. Aucott, H. L. Milton, S. D. Robertson, A. M. Z. Slawin, G. D. Walker, J. D. Woollins, *Chem. Eur. J.* **2004**, *10*, 1666–1676.

[11] S. M. Aucott, P. Kilian, S. D. Robertson, A. M. Z. Slawin, J. D. Woollins, *Chem. Eur. J.* **2006**, *12*, 895–902.

[12] R. Oilunkaniemi, R. S. Laitinen, M. Ahlgrén, *J. Organomet. Chem.* **2001**, *623*, 168–175.

[13] V. K. Jain, S. Kannan, R. J. Butcher, J. P. Jasinski, *J. Organomet. Chem.* **1994**, *468*, 285–290.

[14] V. P. Ananikov, I. P. Beletskaya, G. G. Aleksandrov, I. L. Eremenko, *Organometallics* **2003**, *22*, 1414–1421.

[15] M. Tesmer, H. Vahrenkamp, *Eur. J. Inorg. Chem.* **2001**, 1183–1188.

[16] V. Lippolis, F. Isaia, in: *Handbook of Chalcogen Chemistry, New Perspectives in Sulfur, Selenium and Tellurium* (Ed.: F. A. Devillanova), **2006**, p. 477.

[17] P. D. Boyle, S. M. Godfrey, *Coord. Chem. Rev.* **2001**, *223*, 265–299.

[18] W. Nakanishi, in: *Handbook of Chalcogen Chemistry, New Perspectives in Sulfur, Selenium and Tellurium* (Ed.: F. A. Devillanova), **2006**, p. 644.

[19] S. Ford, P. K. Khanna, C. P. Morley, M. D. Vaira, *J. Chem. Soc., Dalton Trans.* **1999**, 791–794.

[20] S. J. Sabounchei, A. Naghipour, *Molecules* **2001**, *6*, 777–783.

Received: March 31, 2010
Published Online: July 9, 2010

